Denoising Diffusion-Weighted Images by Using Higher-Order Singular Value Decomposition

Xinyuan Zhang[1], Man Xu[1], Zhe Zhang[2], Hua Guo[2], Fan Lam[3], Zhipei Liang[3], Qianjin Feng[1], Wufan Chen[1], and Yanqiu Feng[1]

[1]*Biomedical Engineering, Guangdong Provincial Key Laboratory of Medical Image Processing, Southern Medical University, Guangzhou, Guangdong, China,* [2]*Biomedical Engineering, Center for Biomedical Imaging Research,Tsinghua University, Beijing, Beijing, China,* [3]*Electrical and Computer Engineering, University of Illinois at Urbana-Champaign, Urbana, Illinois, United States*

TARGET AUDIENCE: Clinicians and engineers who are interested in the Diffusion-weighted MRI.

Purpose: Diffusion-weighted (DW) magnetic resonance imaging is widely used in clinic and research because of its ability to characterize the diffusion of water molecules within tissue. However, the DW images are usually affected by severe noise especially at high resolution and high b values, and the low signal-to-noise ratio may degrade the reliability of the subsequent quantitative analysis. Recently, a patch-based higher-order singular value decomposition (HOSVD) method [1] was proposed to denoise MR images and demonstrated to outperform the well-known BM4D method [2]. Compared with the conventional T1-, T2- and proton density (PD)-weighted images, DW images may contain more redundant information because that they are usually highly correlated across different diffusion directions. In this work, we proposed to simultaneously exploit the redundant information along diffusion directions and across spatial domain by using HOSVD in denoising DW images.

Theory: This section describes the HOSVD-based denoising strategy. Given a noisy $(I_1 \times I_2 \times \ldots \times I_N)$-tensor $\mathbf{A}$, its HOSVD can be written as: $\mathbf{A} = \mathbf{S} \times_1 \mathbf{U}^{(1)} \times_2 \mathbf{U}^{(2)} \ldots \times_N \mathbf{U}^{(N)}$, where $\mathbf{S}$ is a $(I_1 \times I_2 \times \ldots \times I_N)$-tensor, $\mathbf{U}^{(n)}$ is a orthogonal unitary matrix and $\times_n$ denotes the n-mode product of a tensor by a matrix $\mathbf{U}^{(n)}$. The smaller HOSVD coefficients in $\mathbf{S}$ usually correspond to contributions from noise. Thus, an estimate of $\mathbf{A}$ with reduced noise can obtained by nullifying the coefficients of tensor $\mathbf{S}$ below a fixed threshold $\tau = \sigma\sqrt{2\log(I_1 \times I_2 \times \cdots \times I_N)}$ and perform inverse HOSVD transform of thresholded tensor: $\hat{\mathbf{A}} = \hat{\mathbf{S}} \times_1 \mathbf{U}^{(1)} \times_2 \mathbf{U}^{(2)} \ldots \times_N \mathbf{U}^{(N)}$, where $\hat{\mathbf{S}}$ is the tensor after thresholding.

Methods: Fig. 1 shows the flow diagram of the proposed method, which consists of two levels of HOSVD: the HOSVD of the whole DW image set and the patch-based HOSVD. Let $\mathbf{Y_n} \in \mathbf{R}^{H \times W \times K}$ denote the noisy DW magnitude images of K directions and with size $H \times W$. The HOSVD denoising of the whole DW image set $\mathbf{Y_n}$ is firstly performed as described in the theory section to obtain prefiltered images $\mathbf{Y_p}$, which will provide more accurate information to guide the patch clustering and the HOSVD of clustered similar patches in the following patch-based HOSVD denoising stage. The patch-based HOSVD considers two characteristics of DW images: sparsity among similar patches across spatial domain and high correlation along diffusion directions. In patch clustering, L similar patches of size $p^2 \times K$ are found for each reference patch by searching and thresholding the photometric distance between two patches, where p^2 denotes the size of neighborhood in the spatial domain. The searching is performed on prefiltered images to mitigate the impact from noise. After that, the similar patches are stacked into a 3D tensor $\mathbf{G_n}$ of size $p^2 \times K \times L$ and then the HOSVD method is implemented to denoise this tensor using the bases trained from the tensor $\mathbf{G_p}$ consisting of patches on the same locations in the prefiltered images. Finally, the denoised patches are aggregated to denoised images. Variance stablization transform and its inverse are implemented to deal with the Rician and non-central Chi noise [1].

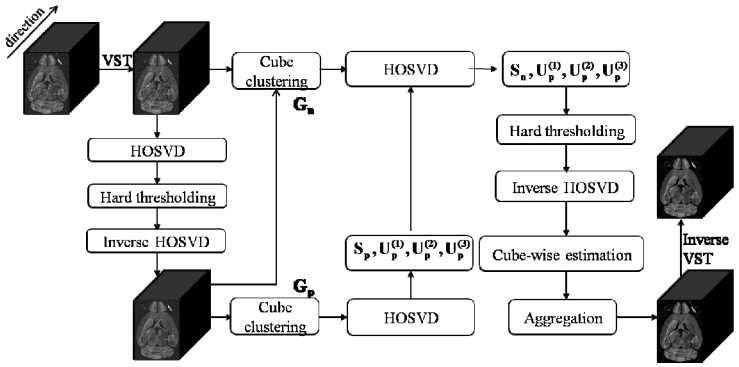

Fig. 1. Flow diagram of the proposed HOSVD alogorithm

We evaluate the proposed method on both simulated and real data. The simulated DW images are from an adult mouse diffusion tensor atlas of size 256×256 consisting of one image with b=0 and 44 images with b=2000s/mm^2 [3]. The real DW data was acquired on a Philips Achieva 3.0T TX MR scanner (Best, Netherlands) with 4-shot EPI sequence using an 8-channel receiver head coil. One image with b = 0 and 6 images with b = 1000 s/mm^2 were acquired with parameters: TR/TE = 3000/82 ms, in-plane resolution = 1× 1 mm^2, slice thickness = 4 mm, matrix size = 220×220, 14 slices, NEX = 10.

Results: Fig. 2 shows the quantitative comparison of the NLM [4], LR+Edge [3] and HOSVD methods on the simulated data using the peak signal to noise ratio (PSNR) of DW images and root-mean-square error (RMSE) of fraction anisotropy (FA), which were calculated only in the anatomical region. It can be observed that HOSVD significantly outperforms NLM and LR+Edge in terms of image PSNR and FA RMSE. Fig. 3 presents the FA maps from the simulated data under a noise level of 5%. Both RL+Edge and HOSVD produce images with reduced noise and well-preserved edges. The FA map from HOSVD-filtered data is smoother and has clearer definition of edges than that from LR+Edge-filtered data. Fig. 4 shows that FA map from the HOSVD-filtered images is less noisy than that from the noisy images and close to the reference FA from the data of NEX = 10.

Conclusion: The proposed HOSVD denoising algorithm has the advantage of simultaneously exploiting redundant information along diffusion directions and across spatial domain. The results on the simulated and real data show that the proposed algorithm can successfully remove noise in DW images while preserving fine details, and thus will benefit the estimation of diffusion-related parameters.

Referances: [1]Zhang et al., MIA, 2015; 19(1):79-86. [2]Maggioni et al., IEEE TIP, 2013; 22(1):119-133. [3]Lam et al., MRM, 2013; 71(3):1272-1284. [4]Wiest-Daessle´ et al., MICCAI2007,10: 344-351.

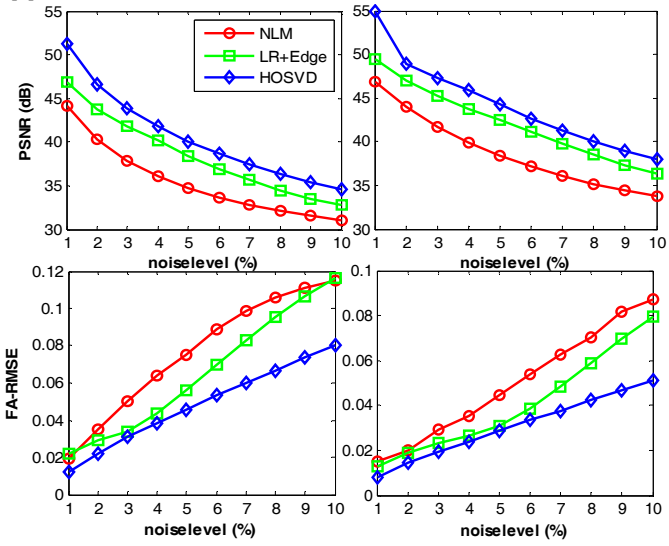

Fig. 2. Quantitative comparison of different denoising methods for Rician distributed data (left) and noncentral-chi distributed data (right).

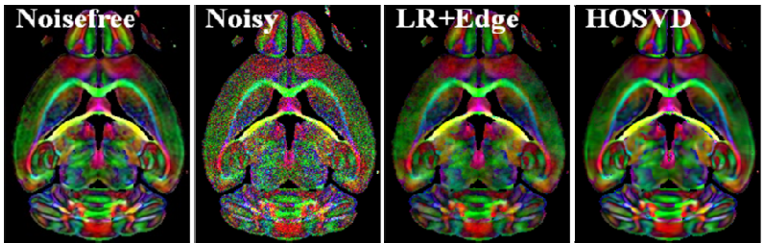

Fig 3. FA maps from simulated data with 5% Rician noise

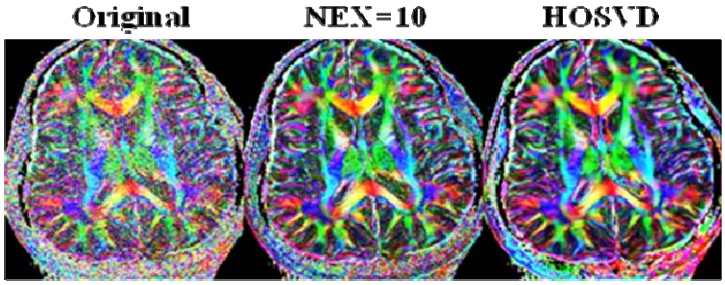

Fig 4. FA maps from the real DW data.